Terahertz emission properties of arsenic and oxygen ion-implanted GaAs based photoconductive pulsed sources

B. Salem, D. Morris,[a] and Y. Salissou
Centre de Recherche en Nanofabrication et Nanocaractérisation (CRN²), Université de Sherbrooke, Sherbrooke, Quebec QC J1K 2R1, Canada
and Département de Physique, Université de Sherbrooke, Sherbrooke, Quebec QC J1K 2R1, Canada

V. Aimez and S. Charlebois
Centre de Recherche en Nanofabrication et Nanocaractérisation (CRN²), Université de Sherbrooke, Sherbrooke, Quebec QC J1K 2R1, Canada
and Département de Génie Électrique et Génie Informatique, Université de Sherbrooke, Sherbrooke, Quebec QC J1K 2R1, Canada

M. Chicoine and F. Schiettekatte
Département de Physique, Université de Montréal, Roger-Gaudry House 2900, Boulevard Édouard-Montpetit, Montreal, Quebec H3T 1J4, Canada

(Received 19 August 2005; accepted 6 February 2006; published 4 May 2006)

In this work we compare the characteristics of asymmetrically excited small-aperture antenna-type pulsed terahertz emitters fabricated using an ion implantation process. Our photoconductive materials consist of high resistivity GaAs substrates. Multienergy implantations of arsenic (1.2 and 2 MeV) and oxygen (180, 450, and 700 keV) have been used to obtain an almost uniform density of vacancies over the optical absorption depth in bulk GaAs substrates. Terahertz pulses are generated by exciting our devices with ultrashort laser pulses. Ion implantation followed by a thermal annealing process introduces nonradiative centers in our substrates which reduce the carrier lifetime and modify the shape of our terahertz pulses. Results obtained as functions of the laser excitation power and bias voltage are discussed and a comparison of the performance of these devices with conventional small-aperture antennas is given. © *2006 American Vacuum Society.* [DOI: 10.1116/1.2183284]

I. INTRODUCTION

Terahertz radiation systems have received much interest in recent years due to their widespread scientific and military applications. The ultra-wide-band and the optical coherence of terahertz pulses also account for considerable efforts made to apply terahertz technology for spectrally determining the optical and electrical properties of crystals, polymers, and organic liquids. Terahertz radiation has been generated by illuminating various emitters, including externally biased photoconductive (PC) antennas, surface built-in field biased semiconductors, and nonlinear crystals with short optical pulses. In the last decade, low-temperature (LT) grown GaAs (Refs. 1 and 2) has been widely used as the substrate of PC antennas for the generation and detection of terahertz radiation. Such materials can be processed to obtain high resistivity ($10^7\ \Omega\,\mathrm{cm}$)[3] and reasonably good carrier mobility ($100-300\ \mathrm{cm^2/V\,s}$),[2,4] in addition to short carrier lifetime (<1 ps).[5,6] These excellent characteristics are however difficult to reproduce from sample to sample because the quality of the material depends critically on both the growth temperature and the postgrowth thermal annealing conditions. An alternative material was reported to be promising as the substrate material of PC antennas, that is, the arsenic ion-implanted GaAs (noted GaAs:As hereafter).[7] These materials exhibit good structural and electrical properties and show ultrafast optoelectronic response. It is again possible to improve the carrier mobility of these ion-bombarded materials using postimplantation thermal annealing process. Good control over the overall fabrication process allows studies of the influence of parameters such as the ion implantation dose, the ion energy, and the thermal annealing conditions on the PC antenna characteristics.

GaAs:As PC antennas have shown to be better terahertz emitters than those made on semi-insulating (SI) GaAs substrates.[8–11] Such enhancement results from ultrafast carrier recombination associated with the presence of the implantation-induced defects. On the other hand, several groups have shown good characteristics of terahertz emitters with the use of PC antennas made on GaAs substrates grown by the Czochralski method when these devices are photoexcited near the anode. A nonuniform electric field between the electrodes of the antenna, resulting from background charge defects (EL2 defects), might explain this result.[12] Although defects seem to play a crucial role in the characteristics of terahertz PC antenna emitters, there are very few studies that investigate the role of defects on these characteristics. Ion implantation using other types of ions has already been used successfully to reduce the carrier lifetime in SI GaAs. For example, subpicosecond lifetime can be obtained in GaAs:H

[a]Electronic mail: denis.morris@usherbrooke.ca

TABLE I. Ion-implantation conditions.

Ion type	Energy (keV)	Doses (cm^{-2})
As	1200	1×10^{12}
	2000	2.5×10^{12}
O	180	0.8×10^{13}
	450	1.2×10^{13}
	700	1.8×10^{13}

and GaAs:O.[13,14] However, few papers report fabrication of antennas on such substrates.

In this paper, we compare the terahertz radiation performance of our PC antenna emitters fabricated on GaAs:As and GaAs:O ion-implanted substrates. We demonstrate broader terahertz bandwidth and higher breakdown voltage for implanted GaAs antennas as compared to SI GaAs antenna.

II. EXPERIMENTAL DETAILS

In this work, we have used commercial high-resistivity ($>10^7\ \Omega$ cm) liquid-encapsulated-Czochralski-grown, (100)-oriented, SI GaAs substrates as starting materials. Our GaAs:As and GaAs:O substrates were then prepared using ion implantation at room temperature. For each substrate, multiple implants using different ion energies have been performed in order to achieve a relatively uniform defect distribution over the implantation depth. Using the SRIM software,[15] the maximum ion implantation depth was estimated to be about 1 μm for both As and O ions, with number of displacements per atoms of less than 0.008 in both cases. The ion implantation conditions for each studied substrates are summarized in Table I. The electrode patterns for the emitters and the detector are fabricated using a conventional photolithography and lift-off. Ohmic contacts were obtained by using a standard mixture of Ni/Au–Ge/Au for the metallization and annealed at around 410 °C for 30 s. The typical size of the PC gap for the emitter/detector is 120 μm/30 μm, respectively. The width of the electrode lines is 10 μm. For the detector we use an H-shaped electrode configuration with a small gap of 5 μm separating the dipole electrodes. The coplanar lines are long enough (>6 mm) to avoid reflection at the line ends. Our GaAs:H detector is fabricated by first bombarding the SI GaAs substrate with protons at a dose of 10^{15} ions/cm^2 and ion energy of 180 keV. This is followed by thermal annealing at 500 °C for 20 min in a furnace under N_2 gas environment and using a GaAs cap to prevent As desorption. The same annealing conditions were used for the fabrication of our emitters on As- and O-implanted materials.

A mode-locked Ti:sapphire laser at a repetition rate of 82 MHz has been used as the excitation source for the generation of broadband terahertz radiation. The laser wavelength was centered at 760 nm and the width of the optical pulses was about 100 fs. The excitation beam, at an average power adjustable from 10 μW to 200 mW, was focused on our PC antennas with a spot size of about 10 μm near the anode. The terahertz radiation was collected and refocused on our detector using a pair of off-axis parabolic mirrors. The electric field of our terahertz pulses has been probed using delayed optical pulses and the GaAs:H PC antenna. The power of the probing beam was about 15 mW and this beam was focused on the detector gap using a 20× microscope lens (we note that we have not used a Si lens to collimate terahertz radiation).

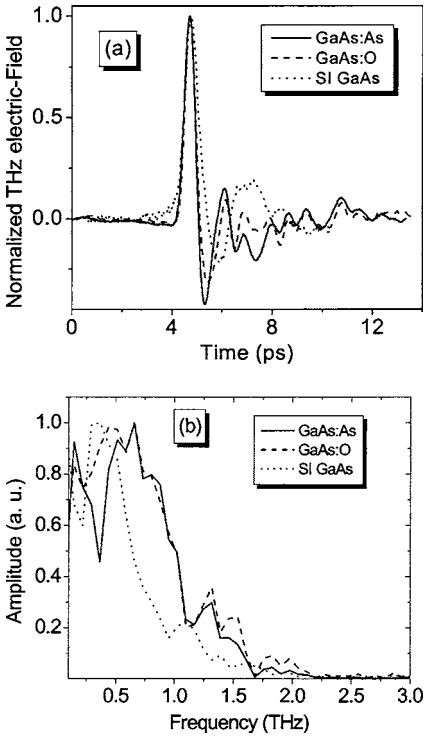

FIG. 1. (a) Amplitude of the terahertz electric field measured using a proton-bombarded GaAs:H PC antenna as detector and a GaAs:As (solid line), a GaAs:O (dash line), or a SI GaAs (dot line) PC antenna as emitter. (b) Fourier transformed amplitude spectra of the GaAs:As (solid line), the GaAs:O (dash line), and the SI GaAs (dot line) terahertz radiation transients shown in (a).

III. RESULTS

The terahertz transient wave forms emitted from the multienergy implanted GaAs:O, GaAs:As, and SI GaAs dipole antennas are shown in Fig. 1. The applied bias voltage and pumping power for the implanted GaAs and the SI GaAs antennas were about 100 V, 90 mW and 40 V, 90 mW, respectively. We observe that the negative peak following the main positive peak is sharper and bigger for the implanted GaAs antenna. Reflecting this difference, the maximum of the Fourier transformed spectra of these electric field transients [Fig. 1(b)] is shifted to a higher frequency compared to that of the SI GaAs antenna. The maximum Fourier component for the GaAs:O and GaAs:As emitters peaks at about 0.9 THz, whereas it peaks at only 0.4 THz for the SI GaAs emitter. The full width at half maximum (FWHM) of the spectrum distribution is about 0.9 THz for multienergy GaAs:As and GaAs:O emitters. To elucidate the observed

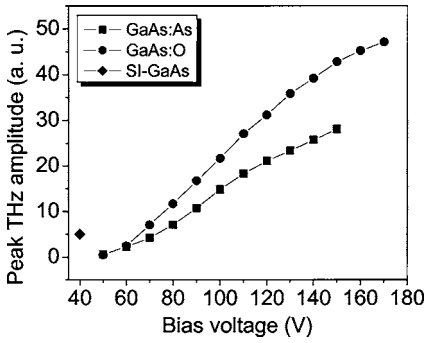

FIG. 2. Amplitude of the terahertz electric field measured as a function of the bias voltage for the GaAs:As PC antenna (square) and for the GaAs:O PC antenna (circle). The pumping power is fixed at 90 mW.

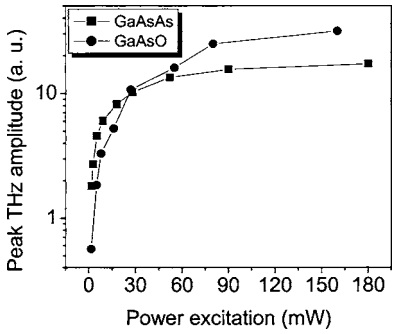

FIG. 3. Amplitude of the terahertz electric field measured as a function of the laser excitation power for our PC antennas made on GaAs:O (circle) and GaAs:As (square) substrates.

difference in the wave forms of the terahertz radiation emitted from the three antennas, we need to consider the carrier dynamics in each photoconductive substrate. In fact, considering the dipole radiation approximation, the main (positive) peak observed in the wave forms in Fig. 1 is attributed to the rise of the surge current by the photocarrier injection and the subsequent carrier acceleration under the bias field in the PC antennas, while the negative peak following the main peak is attributed to the decay of the current governed by the carrier trapping time.[8] The enhanced frequency bandwidth observed for our emitters made on implanted substrates results mainly from a drastic increase of the local electric field induced by the ionization of defects near the anode. This ionization process is driven by the applied bias and the presence of an implantation-induced background of charged defects. Reduction of the carrier lifetime in our implanted materials also contributes to enhance the content of high-frequency Fourier components present in our terahertz pulses.

The terahertz spectrum changes observed in Fig. 1(b) might be more pronounced with the use of an optimal time-domain spectroscopy setup. The water vapor absorption, the width of laser excitation pulses, the absorption and the dispersion of terahertz pulses traversing the GaAs emitter and detector substrates, and the frequency response of the detector are different parameters that can affect the high-frequency roll off of such experimental setup. Although our data are obtained without the use a dry nitrogen purged instrument, we have verified that the terahertz bandwidth of our setup is unchanged under different relative humidity conditions (going from 20% to 50%). Varying the output temporal width of our laser pulses from 150 to 100 fs using the in-cavity prisms of our Ti:sapphire oscillator has almost no effect on our observed terahertz bandwidth. This suggests that it is not our actual frequency bandwidth limitation. Work is under progress in order to further confirm this point by the use of a prechirped and a pulse compressor system to control the temporal shape of our laser pulses at the focal excitation point on our emitter. In order to verify the influence of pulse propagation through the thick substrate of our emitters, we compare the terahertz frequency bandwidth obtained using two different optical setup configurations: collection of the terahertz radiation emitted from either the back or the front surface of our antenna device. Enhanced bandwidth has been reported by Shen *et al.*[16] using the reflection collection mode. In this work, we observe a smaller terahertz signal in the reflection mode configuration, but no modification of the terahertz bandwidth. All these observations suggest that the high-frequency roll off of our experimental time-domain terahertz spectroscopy setup is limited by the frequency response of our detector. Up to now, our terahertz activities focus on the development of devices based on ion-implanted GaAs substrates. We already have varied the implantation and the annealing conditions for obtaining the detector with the largest possible frequency bandwidth. Experiments using other types of ultrafast terahertz detectors (thin electro-optic crystal, LT-GaAs material) need to be performed in order to better characterize the high-frequency performance of our emitters.

To compare the performance of our implanted GaAs emitters, we have also measured the terahertz signals as functions of bias voltage and power excitation. Figure 2 shows the bias voltage dependence of the terahertz intensity measured for our two PC antennas using a constant excitation power of 90 mW, with the laser beam focused near its anode. We have measured these terahertz signals up to a bias level just below the premature breakdown threshold. We observe for both emitters a quadratic increase of the terahertz signal at low biases followed by a saturation regime. The onset value of this saturation regime is correlated to the resistivity of the substrate. High breakdown voltage thresholds >150 V and >170 V are obtained for GaAs:As and GaAs:O antennas, respectively, as compared to 40 V for the SI GaAs PC antenna (not shown here). A high breakdown voltage characteristic is a factor of merit for high-power terahertz radiation sources.

Figure 3 shows the pump power dependence of the peak amplitude in the terahertz wave forms for the GaAs:O and GaAs:As antennas under constant bias voltages of 100 and 110 V, respectively. We clearly observe a saturation regime which occurs at excitation powers greater than 30 mW for the GaAs:As antenna and up to 70 mW for the GaAs:O one. This phenomenon originates from the screening of the local bias field by the photocarriers generated in the gap between of our antenna electrodes.[17]

It is worth mentioning that the results shown in Figs. 2 and 3 are reproducible. We have obtained the same results using a second set of samples implanted on another run. The maximum terahertz signal is still about 1.6 times higher for the GaAs:O emitter than for the GaAs:As emitter. Also the differences observed could not be attributed to other uncontrolled fabrication conditions. We regularly check the reproducibility of our results and never see discrepancies associated with sight drift in these fabrication conditions. All our activities on PC-based terahertz emitters have been largely driven by our capabilities to further improve their characteristics using extremely well controlled ion-implantation conditions.

The difference between the characteristics of these two implanted emitters (GaAs:O and GaAs:As) is attributed to a change in the nature of the defects created by each ion, since their distribution is similar in terms of depth and number of displaced atoms. As implantation generates dense collision cascades compared to the lighter O ions. Each As ion generates nearly ten times more damage than O ions in these experiments. After annealing, defects resulting from As implantation are thus probably more extended and complex, involving a larger number of atoms, while defects induced by O implantation are more sparsely distributed, involving a smaller number of atoms. The latter is apparently more beneficial in terms of carrier recombination control and breakdown voltage since GaAs:O samples feature better emission intensity characteristics at high bias voltages. It is also worth mentioning that molecular dynamics simulations show that in Si, simulation codes using the binary collision approximation such as SRIM underestimate the number of displaced atoms by a factor of nearly 2 for As implantation, while giving a correct estimate for light ion implantation.[18] The amount of damage may thus be larger for As implantation than for O implantation in these experiments, however, similar carrier lifetimes are obtained for both species. A higher breakdown voltage associated with a large number of defects in GaAs is a phenomenon already observed, for instance, in low-temperature grown GaAs.[19] The formation of complex defects, in the case of As bombardment, seems to leave conductive paths through which premature breakdown can occur at high bias voltages.

IV. CONCLUSION

In summary, we have compared the characteristics of our PC antenna emitters fabricated on GaAs:As and GaAs:O ion-implanted substrates. We have shown that our ion-implantation fabrication process favors the emission of intense terahertz radiation. Broadband pulses of almost 1 THz bandwidth and higher breakdown voltage are obtained for these implanted devices. We have pointed out also the high efficiency of the GaAs:O emitter as compared to the GaAs:As one. We have shown that this effect may be due to the nature and the distribution of defect.

ACKNOWLEDGMENTS

This work has received financial support from FEMTOTECH, a research-oriented project supported by "Valorisation-Recherche-Québec." It has been also supported by NSERC, FQRNT, and Nano-Québec. The authors would like to thank the technician and professional staff, Dr. J. Beerens, S. Melançon, M. Lacerte, P. Lafrance, and G. Bertrand, for sample preparation and processing, and Louis Godbout for technical assistance with the accelerator operation. The authors also wish to thank Professor J. Beauvais and Professor D. Houde for valuable discussions on terahertz devices.

[1]M. Tani, S. Matsuura, K. Sakai, and S. Nakashima, Appl. Opt. **36**, 7853 (1997).
[2]M. Tani, S. Sakai, and H. Mimura, Jpn. J. Appl. Phys., Part 2 **36**, L1175 (1997).
[3]F. W. Smith *et al.*, Appl. Phys. Lett. **54**, 890 (1989).
[4]D. C. Look, Thin Solid Films **231**, 61 (1993).
[5]C. Ludwig and J. Kuhl, Appl. Phys. Lett. **69**, 1194 (1996).
[6]S. Kono, M. Tani, and K. Sakai, Appl. Phys. Lett. **79**, 898 (2001).
[7]A. Claverie, F. Namavar, and Z. Liloental-Weber, Appl. Phys. Lett. **62**, 1271 (1993).
[8]T.-A. Liu, M. Tani, and C.-L. Pan, J. Appl. Phys. **93**, 2996 (2003).
[9]G.-R. Lin and C.-L. Pan, Appl. Phys. B: Lasers Opt. **72**, 151 (2001).
[10]J. Lloyd-Hughes, E. Castro-Camus, M. D. Fraser, C. Jagadish, and M. B. Johonston, Phys. Rev. B **70**, 235330 (2004).
[11]T.-A. Liu, M. Tani, M. Nakajima, M. Hangyo, and C.-L. Pan, Appl. Phys. Lett. **83**, 1322 (2003).
[12]S. E. Ralph and D. Grischkowsky, Appl. Phys. Lett. **59**, 1972 (1991).
[13]M. Lambsdorff, J. Kuhl, J. Rosenzweig, A. Axmann, and Jo. Schneider, Appl. Phys. Lett. **58**, 1881 (1991).
[14]M. J. Lederer, B. Luther-Davies, H. H. Tan, C. Jagadish, M. Haiml, U. Seigner, and U. Keller, Appl. Phys. Lett. **74**, 1993 (1999).
[15]J. F. Ziegler and J. P. Biersack, available online at http://www.srim.org
[16]Y. C. Shen, P. C. Upadhya, E. H. Linfield, A. G. Davies, I. S. Gregory, C. Baker, W. R. Tribe, and M. J. Evans, Appl. Phys. Lett. **85**, 164 (2004).
[17]P. K. Benicewicz, J. P. Roberts, and A. J. Taylor, J. Opt. Soc. Am. B **11**, 2533 (1994).
[18]M.-J. Caturla, T. Díaz de la Rubia, L. A. Marqués, and G. H. Gilmer, Phys. Rev. B **54**, 16683 (1996).
[19]J. K. Luo, H. Thomas, D. V. Morgan, and D. Westwood, J. Appl. Phys. **79**, 3622 (1996).